Electron Spin−Echo Envelope Modulation and Pulse Electron Nuclear Double Resonance Studies of $Cu^{2+}\cdots\beta$-Carotene Interactions in Cu-MCM-41 Molecular Sieves

Yunlong Gao,*,† Lowell D. Kispert,*,‡ Johan van Tol,§ and Louis-Claude Brunel§

Key Lab of Analytical Chemistry for Life Science, Department of Chemistry, Nanjing University, Nanjing, 210093, People's Republic of China, Department of Chemistry, BOX 870336, University of Alabama, Tuscaloosa, Alabama 35487, and Center for Interdisciplinary Magnetic Resonance, National High Magnetic Field Laboratory, Florida State University, Tallahassee, Florida 32310

Received: May 15, 2005; In Final Form: July 13, 2005

Perdeuterated all-trans β-carotene imbedded in activated Cu−MCM-41 was examined by electron paramagnetic resonance (EPR) and electron spin−echo envelope modulation (ESEEM) spectroscopies. The EPR study showed that complexation and electron transfer between Cu^{2+} and deuterated β-carotene occurs. The interaction was confirmed by detecting the spin−echo modulation of deuterium in the ESEEM spectra of Cu^{2+}. Ratio analysis of ESEEM was used to determine the number of deuterons which interact with Cu^{2+} and the distance between deuteron(s) and Cu^{2+}. The bonding site of β- carotene determined by ESEEM and pulse electron nuclear double resonance is the C15═C15′ double bond.

Introduction

Carotenoids (Car) serve as light-harvesting and photoprotection agents in photosynthetic centers,[1,2] where they are also involved in electron transfer (ET) resulting in carotenoid radical cations ($Car^{\bullet+}$).[3] To understand the photophysical properties of Car, ET reactions of Car in various heterogeneous hosts have been studied.[4−6]

Recently, ET reactions of Car imbedded in mesoporous molecular sieves MCM-41 and metal ion substituted MCM-41 (Ni−MCM-41,[7] Al−MCM-41,[7] Fe−MCM-41,[8] Ti−MCM-41,[9] and Cu−MCM-41[10]) have been studied. MCM-41 is a mesoporous silica containing a regular array of uniform cylindrical pores. The pore size ranges from 15 to 100 Å depending on the chain length of the template used in the synthesis.[11] Previous studies[7−10,12,13] have shown that such materials provide a microenvironment appropriate for retarding back ET and increasing the lifetime of photoproduced radical ions. Some carotenoids, such as β-carotene imbedded in transition metal ion substituted MCM-41 (Ti−MCM-41 and Cu−MCM-41), interact with the transition-metal ions and form a complex.[9,10] The bonding in a transition-metal−olefin complex is often described by the Dewar−Chatt−Duncanson model:[14,15] electron donation from a filled π orbital of an olefin into vacant s, p, or d orbitals of the metal and binding overlap between an occupied d orbital of metal with the empty π^* orbital of the olefin (π back donation). Formation of the Cu^{2+}−Car complex favors light-driven ET from Car to Cu^{2+} and also permits thermal back ET from Cu^{+} to $Car^{\bullet+}$.[10]

However, previous studies could not ascertain which double bond(s) of carotenoids interact(s) with metal ions nor determine the distance between Car and the metal ion in the complex. This information is important for the analysis of the distance-dependent reversible ET between Car and metal ions. In this study, electron spin−echo envelope modulation (ESEEM) experiments were performed with perdeuterated all-trans β-carotene (**I**) (Chart 1) imbedded in Cu−MCM-41. Ratio analysis of ESEEM showed that Cu^{2+} interacts with two deuterons at a distance of 3.3 Å. Pulse electron nuclear double resonance (ENDOR) was also used to determine which double bond interacts with Cu^{2+}. The short distance between **I** and Cu^{2+} explains why reversible ET occurs.

Experimental Section

Chemicals. Fully deuterated all-trans β-carotene (**I**) was kindly donated by the Argonne National Laboratory, where it was extracted from 99% deuterated *Scenedesmus obliquus* algae.[16] All-trans nondeuterated β-carotene, purchased from Fluka, was purified by extraction with benzene and precipitation with methanol. Anhydrous dichloromethane was from Aldrich.

Synthesis of Cu−MCM-41 and Electron Paramagnetic Resonance (EPR) Sample Preparation. The procedures for synthesis of Cu−MCM-41 and EPR sample preparation are described in ref 10.

EPR. X-band EPR measurements were carried out with an X-band (9.5 GHz) Varian (Palo Alto, CA) E-12 EPR spectrometer, equipped with a rectangular cavity. The magnetic field was measured with a Bruker (Billerica, MA) EPR 035M gaussmeter, and the microwave frequency was measured with a model HP 5245L frequency counter.

ESEEM and Pulse ENDOR. ESEEM and pulse ENDOR experiments were carried out with a Bruker ELEXSYS E580 FT/CW pulse X-band EPR spectrometer.

Results and Discussion

EPR spectra of activated Cu−MCM-41 alone and those with adsorbed nondeuterated β-carotene have been reported.[10] The spectrum of the activated Cu−MCM-41 showed an orthorhombic geometry of Cu^{2+} with $g_{xx} = 2.07$, $g_{yy} = 2.13$, and $g_{zz} = 2.49$. The EPR spectrum changed significantly after β-carotene was imbedded in Cu−MCM-41. Two species were detected.

* To whom correspondence should be addressed. E-mail: gao003@bama.ua.edu (Y.G.); lkispert@bama.ua.edu (L.D.K.).
† Nanjing University.
‡ University of Alabama.
§ Florida State University.

10.1021/jp052550v CCC: $30.25
Published on Web 09/10/2005

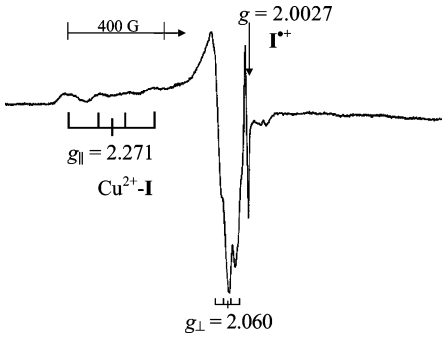

Figure 1. EPR spectrum (77 K) of Cu−MCM-41 with adsorbed **I**.

CHART 1

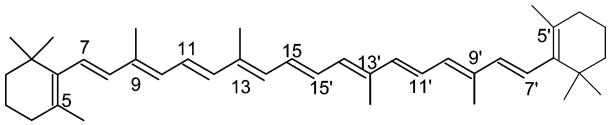

(**I**)

One is Cu^{2+} with hyperfine splitting in the $g_\perp$ and $g_{||}$ regions, and the other is the β-carotene radical cation (Car•$^+$) formed by oxidation[10] of β-carotene by Cu^{2+}

$$\text{Car} + \text{Cu}^{2+} \rightleftharpoons \text{Car}^{\bullet+} + \text{Cu}^{+} \qquad (1)$$

The EPR spectrum (Figure 1) after **I** was imbedded in the activated Cu−MCM-41 also shows that there are two species. One is the Cu^{2+} EPR signal with $g_{||} = 2.271$, $g_\perp = 2.060$, $A_{||} = 0.0172$ cm^{-1}, and $A_\perp = 0.0026$ cm^{-1} (A is the hyperfine constant) and is due to the Cu^{2+}−Car complex, in which Cu^{2+} has a tetrahedral geometry.[10] The other, with $g = 2.0027$ is assigned to the radical cation of **I** (**I**•$^+$), formed by oxidation of **I** by Cu^{2+}. The g value of **I**•$^+$ is the same as that of the radical cation produced when nondeuterated β-carotene was imbedded in Cu−MCM-41.[10] However, the peak to peak line width ΔH_{pp} of **I**•$^+$ (8 G) is much narrower than that of nondeuterated β-carotene radical cation (line width about 14 G[10]) because deuteron coupling is smaller than that of proton.[17]

To obtain echo intensity decay with a resolvable modulation for a three-pulse ESEEM spectrum, the perdeuterated β-carotene must be studied. An ESEEM spectrum of nondeuterated β-carotene will not have a resolvable modulation since the proton frequency is approximately 6 times larger.[18] The three-pulse ESEEM spectrum (Figure 2) was recorded in the $g_\perp$ spectral region of the Cu^{2+}−**I** powder spectrum. The signal intensity is proportional to the square root of the power because phase sensitive detection was used. Interfering two-pulse echoes were suppressed by phase-cycling techniques. Ratio analysis of ESEEM was carried out by the method developed by Ichikawa et al.[19] The method can be applied to systems with n equivalent nuclei. The data analysis proceeds by comparing the experimental ratios

$$R_{\text{exp}}(t) = V_{\text{max,exp}}(t)/V_{\text{min,exp}}(t) \qquad (2)$$

(where V is the echo intensity) with the theoretical ratios

$$R_{\text{th}}(t) = [R_1(t,r,a)]^n \qquad (3)$$

where t can be T or τ, depending on whether three- or two-pulse data are being analyzed, R_1 (the theoretical ratio for a single nucleus) is a function of t, r is the distance from the radical (Cu^{2+} in this case) and one nucleus (D in this case), and a is the coupling constant. To obtain R_{exp}, curves are drawn

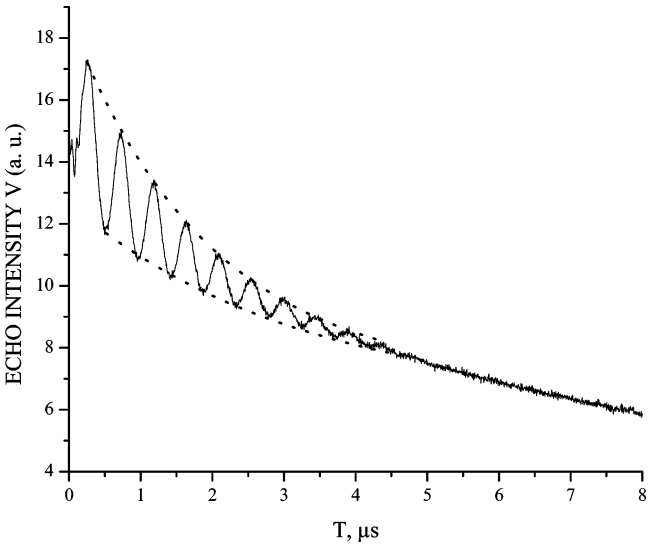

Figure 2. Three-pulse ESEEM of Cu−MCM-41 with adsorbed **I**. Field setting on Cu^{2+} perpendicular region at 20 K. V is proportional to the square root of the microwave power. Curves have been drawn through the maxima and minima of the nuclear Zeeman interaction component (ω_I) of the echo modulation to aid in the analysis.

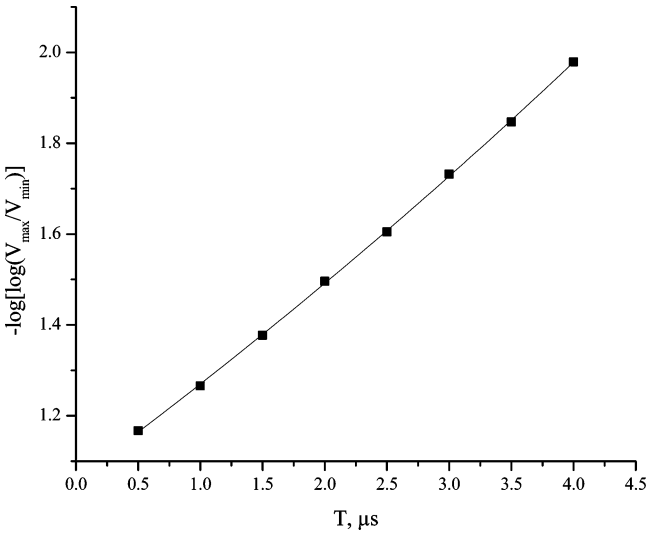

Figure 3. Ratio analysis of three-pulse ESEEM of Cu−MCM-41 with adsorbed **I**.

through the maxima and minima of the nuclear Zeeman interaction component (ω_I) of the echo modulation (Figure 2). Since

$$R_{\text{exp}} \approx R_{\text{th}} = [R_1(t,r,a)]^n \qquad (4)$$

Taking loglog of eq 4 gives

$$\text{Loglog}(R_{\text{exp}}) \approx \log(n) + \text{loglog}(R_1) \qquad (5)$$

In the loglog(R_{exp}) and loglog(R_1) plots vs T (three-pulse) or τ (two-pulse), a and r can be chosen to obtain the most nearly parallel curves. The separation between the two curves is log(n).[19] In the calculation, the experimental data [loglog(R_{exp}), T] were first entered into the computer, and then the eq 5 was entered into the computer as the function to fit the experimental data. After fitting, the computer displays the best nonlinear least-squares fit parameters (n, a, and r).

Figure 3 shows the best nonlinear least-squares fit of the three-pulse data obtained with the parameters listed in Table 1, which

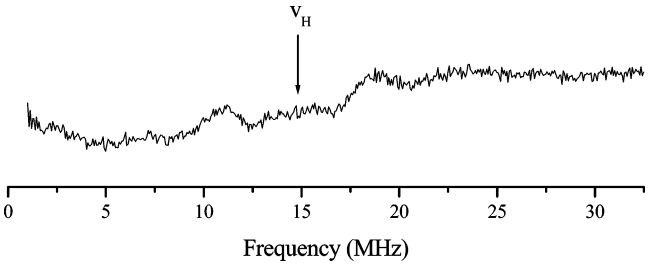

Figure 4. Pulse ENDOR spectrum of β-carotene radical cation in Cu−MCM-41.

TABLE 1: Best Nonlinear Least-Squares Fit Parameters for Cu^{2+}−I Complex in Cu−MCM-41

T range (μs)	*r* (Å)	*n*	*a* (MHz)
0.50−4.0	3.3 (0.2	2.2 (0.1	0.06 (0.2

show that Cu^{2+} interacts with two deuterons at a distance of 3.3 Å between Cu^{2+} and deuteron, which is similar to the reported distance[20] for the interaction between Cu^{2+} and other small deuterated molecules, such as D_2O and CH_3OD, in MCM-41. Because application of the ratio analysis method is based on the assumption that *n* nuclei are equivalent, the distance 3.3 Å can be treated as an average of the distances between Cu^{2+} and the two deuterons. Possible double bonds of **I** substituted with one deuterium at each carbon that could interact with Cu^{2+} are C7═C8, C11═C12, C15═C15′, C12′═C11′, and C8′═C7′. Since steric hindrance by the terminal bulky trimethyl cyclohexene rings precludes attainment of the requisite distance between Cu^{2+} and the C7═C8 and C8′═C7′ double bonds, the possible double bonds that could interact with Cu^{2+} are C15═C15′ or C11═C12 (C12′═C11′).

Pulse ENDOR[21,22] can provide information about the orientation of $Car^{\bullet+}$ on solid supports. For example, the ENDOR powder spectrum of the radical cation of β-carotene on activated silica−alumina solid support[22] at 120 K, gave rise to detectable ENDOR lines at 1.9, 8.3, and 13.0 MHz attributed to couplings with the C(5), C(9), and C(13) methyl protons. This assignment was based on calculated proton coupling constants using the RHF-INDO/SP method. It was found that the experimentally observed and the calculated ENDOR spectral line width varied depending on whether the CH_3 group was rapidly rotating (narrow resolved lines appeared for the C(5) and C(9) methyl groups) or a barrier to rotation existed due to nearest neighbors (broad lines for the C(13)-methyl group) that may prevent detection of lines due to the (C13) methyl group. The influence of the surroundings on the rotation barrier of the methyl groups was clearly evident in the ENDOR spectrum of the radical cation of canthaxanthin in aluminum substituted MCM-41 molecular sieves.[21] In this case, the C(5) and C(9) methyl groups gave rise to very broad, barely detectable lines while the ENDOR lines for the C-13−methyl group gave very sharp narrow and intense peaks. Thus, the line width of the ENDOR spectral lines can be used to qualitatively measure the hindering environment surrounding the radical cations. This broadening is due to the large anisotropy of the methyl group protons (line broadening from incomplete averaging of the methyl proton couplings), which averages out upon rapid rotation, resulting in narrow ENDOR lines. In the pulse ENDOR spectrum of nondeuterated β-carotene radical cation produced in Cu−MCM-41 (Figure 4) peaks due to coupling of C (9 and 9′) CH_3 protons[22] are detected, indicating that the C (9 and 9′) methyl groups are located away from the surface of the pore. Since peaks due to the couplings of C (13 and 13′) are not detected, the middle of the chain of β-carotene interacts with the surface as shown in Figure 5. These

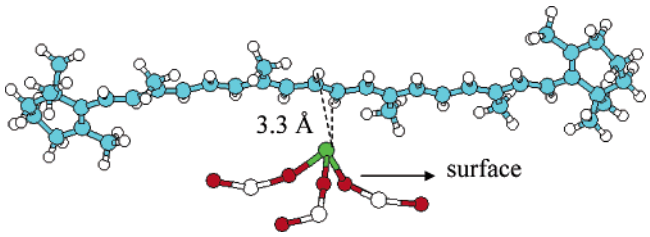

Figure 5. Interaction between Cu^{2+} and β-carotene in Cu−MCM-41: blue, C; green, Cu; red, O; white (large), Si; white (small), H.

results suggest that C15═C15′ not C11═C12 (C12′═C11′) interacts with Cu^{2+}. Because Cu^{2+} interacts with two deuterons at a distance of 3.3 Å between Cu^{2+} and deuteron, the calculated distance between Cu^{2+} and the center of the double bond is about 2.8 Å. This short distance explains why formation of the Cu^{2+}−Car complex favors electron transfer. It is interesting to note that the distance between deuterated ethylene and Cu^{2+} on a silica surface is 3.8 Å,[23] considerably larger than that observed for β-carotene and Cu^{2+} in MCM-41.

Conclusions

ESEEM and pulse ENDOR studies of Cu^{2+}−Car complex in Cu−MCM-41 provide new information about the interaction between the transition-metal ion and carotenoids. Cu^{2+} interacts with the centrally located double bond C15═C15′. The short distance (∼2.8 Å) between the transition-metal ion and β-carotene explains why reversible electron transfer readily occurs. This study also shows that the ratio analysis method is a powerful tool for the interpretation of ESEEM spectra and the determination of the geometry of complexes of paramagnetic metal ions and deuterium-containing compounds.

Acknowledgment. We would like to thank Dr. E. Hand for helpful suggestions. This work was supported by the Division of Chemical Sciences, Office of Basic Energy Sciences, Office of Energy Research of the U.S. Department of Energy under Grant No. DE-FG02-86ER13465.

References and Notes

(1) Koyama, Y. *J. Photochem. Photobiol. B* **1991**, *9*, 265.
(2) Koyama, Y.; Kuki, M.; Andersson, P. O.; Gillbro, T. *Photochem. Photobiol.* **1996**, *63*, 243.
(3) Faller, P.; Pascal, A.; Rutherford, A. W. *Biochemistry* **2001**, *40*, 6431.
(4) He, Z.; Kispert, L. D.; Metzger, R. M.; Gosztola, D.; Wasielewski, M. R. *J. Phys. Chem. B* **2000**, *104*, 6302.
(5) He, Z.; Kispert, L. D. *J. Phys. Chem.* **1999**, *103*, 9038.
(6) He, Z. Ph.D. Dissertation, The University of Alabama, 2000.
(7) Konovalova, T. K.; Gao, Y.; Schad, R.; Kispert, L. D.; Saylor, C. A.; Brunel, L.-C. *J. Phys. Chem. B* **2001**, *105*, 7459.
(8) Konovalova, T. A.; Gao, Y.; Kispert, L. D.; van Tol, J.; Brunel, L.-C. *J. Phys. Chem. B* **2003**, *107*, 1006.
(9) Gao, Y.; Konovalova, T. A.; Xu, T.; Kispert, L. D. *J. Phys. Chem. B.* **2002**, *106*, 10808.
(10) Gao, Y.; Konovalova, T. A.; Lawrence, J. N.; Smitha, M. A.; Nunley, J.; Schad, R.; Kispert, L. D. *J. Phys. Chem. B* **2003**, *107*, 2459.
(11) Beck, J. S.; Vartuli, J. C.; Roth, W. J.; Leonowicz, M. E.; Kresge, C. T.; Schmit, K. D.; Chu, T.-W.; Olson, D. H.; Shepperd, E. W.; McCullen, S. B.; Higgins, J. B.; Schlenker, J. L. *J. Am. Chem. Soc.* **1992**, *114*, 10834.
(12) Krishna, R. M.; Prakash, A. M.; Kevan, L. *J. Phys. Chem. B* **2000**, *104*, 1796.
(13) Sung-Suh, H. M.; Luan, Z.; Kevan, L. *J. Phys. Chem. B* **1997**, *101*, 10455.
(14) Dewar, M. J. S. *Bull. Soc. Chim. Fr.* **1951**, *C79*, 18.
(15) Chatt, J.; Duncanson, L. A. *J. Chem. Soc.* **1953**, 2939.
(16) Strain, H. H.; Thomas, M. R.; Crespi, H. L.; Blake, M. I.; Katz, J. J. *Ann. N. Y. Acad. Sci.* **1960**, *84*, 617.
(17) Reddoch, A. H.; Dodson, Charles L.; Paskovich, D. H. *J. Chem. Phys.* **1970**, *52*, 2318.

(18) Kevan, L. In *Modern Pulsed and Continuous Wave Electron Spin Resonance*; Kevan, L., Bowman, M. K., Eds.; John Wiley & Son: New York, 1990; Chapter 5, pp 231−266.

(19) Ichikawa, T.; Kevan, L.; Bowman, M. K.; Dikanov, S. A.; Tsvetkov, Y. D. *J. Chem. Phys.* **1979**, *71*, 1167.

(20) Xu, J.; Yu, J.-S.; Lee, S. J.; Kim, B. Y.; Kevan, L. *J. Chem. Phys.* **2000**, *104*, 1037.

(21) Konovalova, T. K.; Gao, Y.; Schad, R.; Kispert, L. D.; Saylor, C. A.; Brunel, L.-C. *J. Phys. Chem. B* **2001**, *105*, 7459.

(22) Jeevarajan, A. S.; Kispert, L. D.; Piekara-Sady, L. *Chem. Phys. Lett.* **1993**, *209*, 269.

(23) Ichikawa, T.; Yoshida, H.; Kevan, L. *J. Chem. Phys.* **1982**, *88*, 881.